Role of interparticle forces and interparticle friction on the bulk friction in charged granular media subjected to shearing

S. J. Antony and M. A. Sultan
Institute of Particle Science and Engineering, University of Leeds, LS2 9JT, United Kingdom
(Received 28 June 2006; revised manuscript received 6 October 2006; published 27 March 2007)

We study the consequences of the interplay between electrostatic forces, mechanical contact forces, and frictional properties of grains upon the bulk frictional properties of charged granular media subjected to quasistatic shearing. We show that, the variations in short-range electrostatic forces between the grains (which are often ignored in the existing studies) dominantly affect the bulk friction. Charging enhances the fabric anisotropy of heavily loaded contacts—this enhances the bulk friction, more significantly, in the case of low frictional granular systems.

DOI: 10.1103/PhysRevE.75.031307 PACS number(s): 45.70.−n, 46.55.+d, 47.10.ab

Granular materials behave differently both from ordinary molecular fluids when they flow and from ordinary solids when they remain at rest [1,2]. Fundamental understanding on the collective behavior of particulate systems under combined electromechanical loading environments is sought in several interdisciplinary applications. A few examples are, in the design of electrostatic granular valves, piezoelectric powder compacts/sensors, electromechanical separators for minerals and ores, powder injectors, and microbial particulate fuel cells [e.g., [3–7]]. The developments in micro/nano technologies are pushing the limits of miniature particulate fabrications by designing particle interfaces with enhanced functionalities. This is achieved by precisely controlling the nature of interparticle forces acting between particles [7]. Further, Ambient Intelligence (AmI) and Virtual Process Creation Tools (VPCT) are expected to aid our classrooms in the future [8]. Design of AmI for granular media under combined loading environments should be on the one hand simple (computationally less expensive), and on the other hand should not compromise the physics that govern the collective behavior of granular media. The speed of simulations for granular systems largely depends on the interparticle force-separation models used. Hence, a clear understanding of the roles played by force components will help us to deduce the (normally) nonlinear terms in their force-separation relations, as appropriate. Existing literature on the mechanical and electrostatic phenomena in granular systems are exhaustive [e.g., [3–7]], but our understanding of the mechanics and physics behind the collective behavior of granular systems subjected to combined electromechanical loading conditions is as of yet, limited. In this work, we attempt to answer certain aspects of this problem—the effects of the interplay between the individual interparticle force components in charged systems, such as, the short-range and long-range electrostatic forces, the mechanical contact forces, and the pull-off force between cohesive particles, on the micro-macroscopic characteristics. Are all the interparticle force components contribute to the bulk friction in charged granular systems? What is the effect of interparticle friction on the bulk friction in charged granular systems? We aim to get some answers to these vital questions here, by studying the micromechanical behavior of granular systems in a charged environment in a systematic way using computer simulations.

In this study, we used particle-based Discrete Element Method (DEM) [9–14] to simulate the micromechanical characteristics of charged systems, by appropriately implementing the interparticle force-separation relation between the cohesive particles subjected to electromechanical loading conditions. That is to say, in the interparticle force model, in addition to the electrostatic forces, the mechanical forces acting between the particles are also accounted. Let us consider two dielectric spherical particles (equal size) at a separation distance, r, from each other. The applied detaching electric field is assumed to be in the (perpendicular) direction 3-3 [insert in Fig. 1(a)]. In general, the net electrostatic force (F_{NE}) on a charged particle in an applied electric field (with a fixed electric strength, E), assuming that the charge is distributed uniformly on the surface of a particle, can be written as a sum of four components [5,6]: (i) $-\alpha\frac{Q^2}{16\pi\epsilon_0 r^2}$, (ii) βQE, (iii) $-\gamma\pi\epsilon_0 R^2E^2$ and (iv) $-\kappa W_A\pi R^*$, where Q is the net particle charge, ε_0 is the permittivity of free space given as 8.854×10^{-12} Nm^2/C^2 and α, β, and γ are correction factors, which depend on the polarization of the dielectric particle [6]. These dimensionless coefficients are the functions of dielectric constant of the particle, the particle permittivity and geometric configuration, such as particle size ratio, distance between the particles and the electrodes [6,15,16]. W_A represents the work of adhesion [17]. $\kappa=3/2$, 2 according to the Johnson, Kendall, and Roberts (JKR) and Derjaguin, Muller, and Toporov (DMT) theories, respectively [17]. For the case of same size particles, the reduced radius R^* is equal to half the radius of the particle R [5,17]. The first term represents the electrostatic adhesion due to the attraction between the net charges on the particle and its image charge in the electrode and this also accounts for the variation in the short-range electrostatic force (as a function of separation distance between the particles, $r\leq R$). Existing studies often ignore the variation in short-range force contribution [18]. The second term represents the Coulomb force due to the external field acting on the particle charge and this term accounts for the long-range contribution of electrostatic forces. The third term accounts for the long-range contribution of electrostatic force due to electrostatic adhesion arising from the attraction between the field-induced dipole in an uncharged particle in an electric field and its dipole image [6]. In order to evaluate the magnitude of electrostatic forces, the value of dimension-

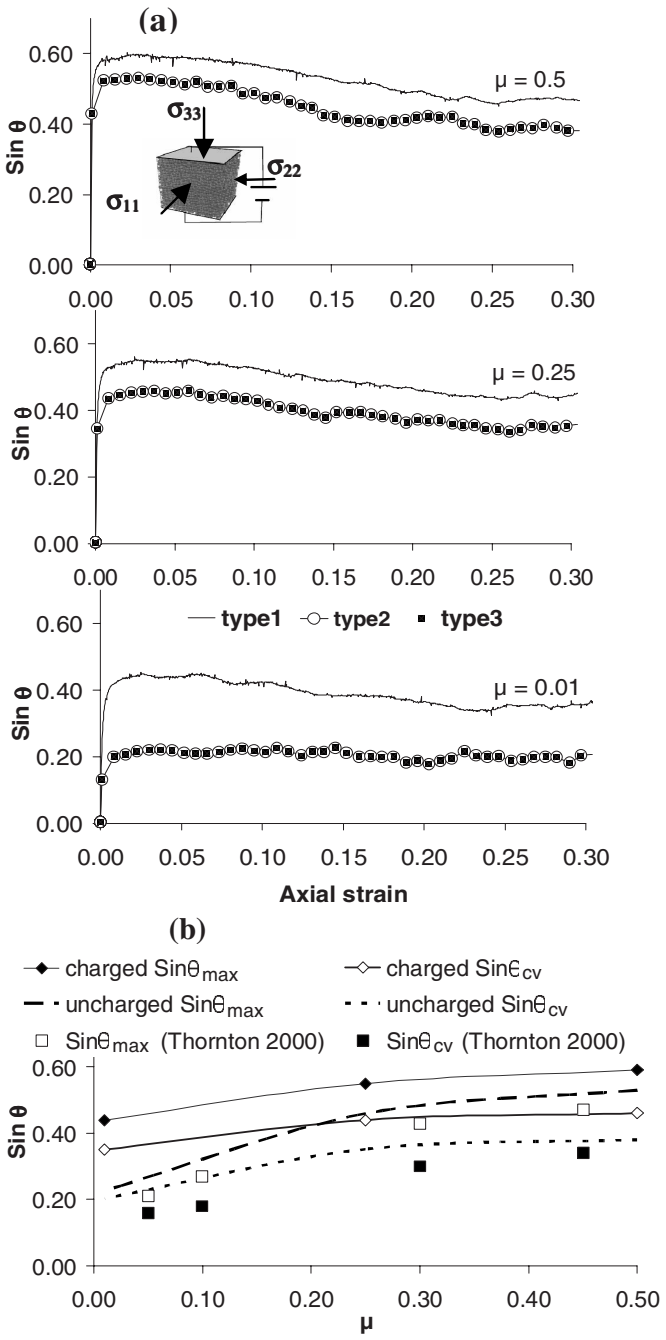

FIG. 1. (a) The evolution of macroscopic friction (sin θ) during shearing. The insert is a schematic diagram of a charged granular assembly subjected to triaxial compression. (b) Effect of interparticle friction on the peak (max) and steady state (cv) values of bulk friction.

less coefficients α, β, and γ is usually solved by the Laplace equation in bispherical coordinates or by the multipole expansion method [19,20]. The dimensional coefficients used here are based on the work of Feng and Hays using Galerkin-finite element method for particles of dielectric constant equal to three [6]. The fourth term represents the pull-off force (van der Waals force) based on either the JKR or DMT theories. The net electrostatic force-separation relation (F_{NE}) is used in our simulations to govern the dynamics of grains in charged granular assemblies. However, when the particles physically touch/overlap, the mechanical forces are computed in the classical way [9] and combined with the electrostatic forces. A simple force mechanism was employed between contacting particles: equal values of linear normal and tangential contact springs were assigned and slipping between particles would occur whenever the specified contact friction coefficient was attained. In short, the simulations consider the combination of linear and nonlinear force-separation models [14] for the contact (mechanical) and noncontact (electrostatic) regimes, respectively.

The particle arrangements were initially random, isotropic, and homogeneous. The assemblies, each contained about 2000 monosized spherical particles in dense packing (initial solid fraction 0.6511), density of particle $\rho_p = 1000\ \mathrm{kg/m^3}$ and the work of adhesion $W_A = 0.08\ \mathrm{J/m^2}$. Consider the particles which have a diameter 10 μm, at a fixed electric strength of $E = 3 \times 10^5$ N/C, and the net charge $Q = 14.52$ fC [6]. The mechanical boundary conditions (shearing) were pertaining to a triaxial compression test: the height of the assembly was slowly reduced at a constant rate along the 3-3 (axial) direction, while maintaining a constant horizontal stress along the 1-1 and 2-2 directions [insert in Fig. 1(a)]. The axial strain was advanced in small increments of $\Delta\epsilon_{33} = 1.0 \times 10^{-5}$. To investigate the effect of interparticle friction (μ) on the bulk friction in charged granular systems, μ was varied as 0.5, 0.25, and 0.01. To investigate the effect of short range and long range electrical forces and the pull-off forces between the particles on the bulk friction, three types of simulation were considered: **Type-1**, which accounted for the variation in the short range electrostatic forces (i.e., F_{NE} is the sum of all the four terms, explained above); **Type-2**, which ignores the variation in short-range electrostatic forces (i.e., F_{NE} is same as in Type-1, except that r is nonvarying. That is to say that r is independent of the separation distance, and approximated by substituting $r = R$ in the first term [18]); **Type-3**: The short range and long range electrostatic forces are ignored, but the pull-off force (term 4) was considered (i.e., pertaining to an uncharged system). In all these different types of simulations, once the neighboring particles touch/overlap, mechanical contact forces are automatically accounted as explained above [14]. The pull-off force between the particles was computed based on the JKR theory. [However, for comparison purposes, all the above tests were repeated by replacing the JKR pull-off force wherever we used, by that of based on DMT theory—we observed no significant differences in our results. Hence, for providing clarity, we do not include the results of DMT theory based simulations in the plots presented below.]

Figure 1(a) shows the evolution of macroscopic (bulk) friction in charged granular assemblies subjected to shearing. The bulk friction is presented in terms of $\sin\theta = (\sigma_{33} - \sigma_{11})/(\sigma_{33} + \sigma_{11})$, ($\sigma_{ij}$, $i = j$ are principal stress components). The results show that, accounting for the contribution of short-range electrostatic force (type 1) results in a significant increase in the value of the bulk friction in charged granular systems. Further, the evolution of macroscopic friction obtained from the type-2 and type-3 simulations is fairly identical, suggesting that the long-range electrostatic forces do not contribute significantly to the bulk

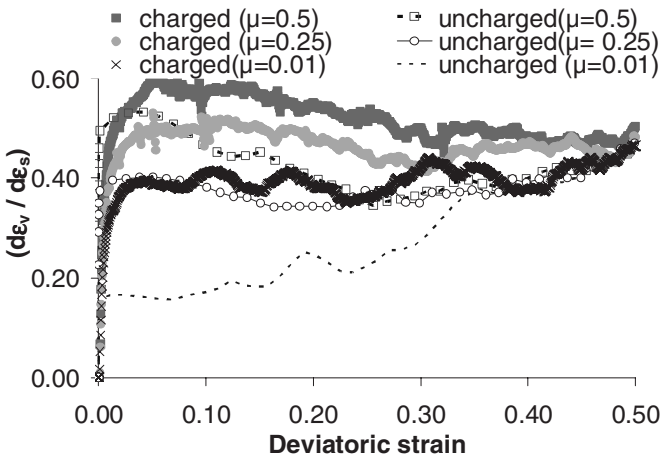

FIG. 2. Evolution of dilation rate $(d\varepsilon_v/d\varepsilon_s)$ during shearing.

friction in charged assemblies studied here. Hence, in the following discussion, we only compare the results between the type-1 and type-3 simulations, henceforth referred to as "charged" and "uncharged" systems, respectively. Figure 1(b) shows the influence of interparticle friction (μ) on the bulk friction, typically at the peak $(\sin\theta_{\max})$ and steady state $(\sin\theta_{cv})$. For an increase in the value of interparticle friction, the bulk friction increased in both the charged and uncharged assemblies. For the purposes of comparison, in Fig. 1(b), we have superimposed the values of bulk friction according to Thornton [21], measured for the uncharged dense (cohesive) granular assemblies. In Thornton's simulations, the cohesive forces are modeled based on the JKR theory [21]. Qualitatively, our simulation results for the uncharged granular systems agree with the trend of the results reported by Thornton [21]. The quantitative differences could be attributed to the differences in the test materials used in the studies (Thornton's results correspond to glass bead assemblies, while the material properties used in our simulations correspond to toner beads).

Figure 2 shows the evolution of the dilation rate $d\varepsilon_v/d\varepsilon_s$ in the assemblies during shearing (ε_v is the volumetric strain $\varepsilon_{11}+\varepsilon_{22}+\varepsilon_{33}$, and ε_s is the deviatoric strain $(2/3)\sqrt{[(\epsilon 11-\epsilon 22)^2+(\epsilon 22-\epsilon 33)^2+(\epsilon 33-\epsilon 11)^2]}$). For a given value of interparticle friction, dilation rate in a charged system is generally higher than that of an uncharged system. From Fig. 2 we can also conclude that, irrespective of whether granular systems are charged or uncharged, they tend to attain a unique value of dilation rate at a large value of deviatoric strain (steady state). Figure 3(a) shows the evolution of contact fraction (i.e., ratio of number of contacts to the initial number of contacts), while Fig. 3(b) shows the sliding fraction (i.e., the ratio between the number of contacts sliding to the total number of contacts at a given value of axial strain). For a given value of inter-particle friction, the charged system presents a higher value of contact fraction, compared with the uncharged system, throughout shearing. For a decrease in the value of interparticle friction, both the contact fraction and sliding fraction tend to increase. The fluctuations in the variation of sliding fraction in charged granular systems tend to diminish (relatively) as the interparticle friction increases. In general, friction enhances rigidity of contacts in both the charged and uncharged [22] granular systems. We observed that the systems that ignore the variation in short-range forces (type-2 and type-3) tend to present relatively a more uniform variation in the sliding fraction.

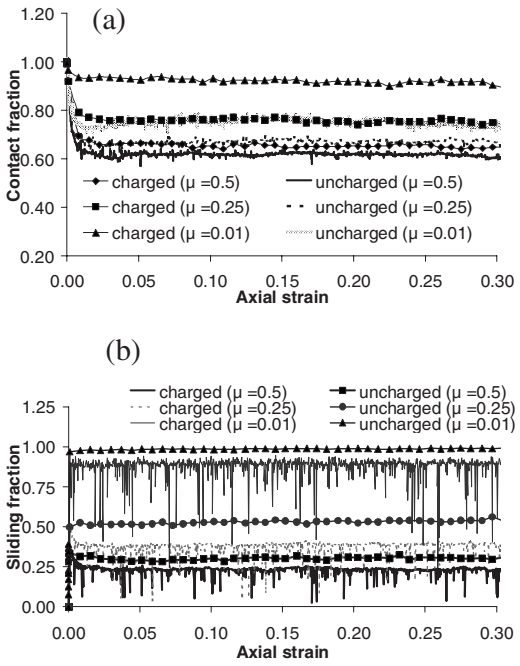

FIG. 3. Evolution of (a) contact fraction and (b) sliding fraction during shearing.

To investigate the charging efficiency in frictional systems, we define two key gain indices, namely, $I_{\sin\theta}=(\sin\theta_{\text{charged}}-\sin\theta_{\text{uncharged}})/\sin\theta_{\text{uncharged}}$ and $I_{\varnothing s}=(\varnothing_{s\ \text{charged}}-\varnothing_{s\ \text{uncharged}})/\varnothing_{s\ \text{uncharged}}$. $\varnothing\ s$ correspond to the fabric anisotropy tensor of heavily loaded contacts. Their values measured at the peak (max) and steady states (cv) are presented in Fig. 4. For a moment, let us concentrate on $I_{\sin\theta}$. We will discuss about $I_{\varnothing s}$ later. From Fig. 4, we observe that, the effect of charging on bulk friction is more dominant in assemblies with low values of interparticle friction $(\mu<0.25)$. To investigate the underlying physics behind the increase in bulk friction in charged systems, we probed the

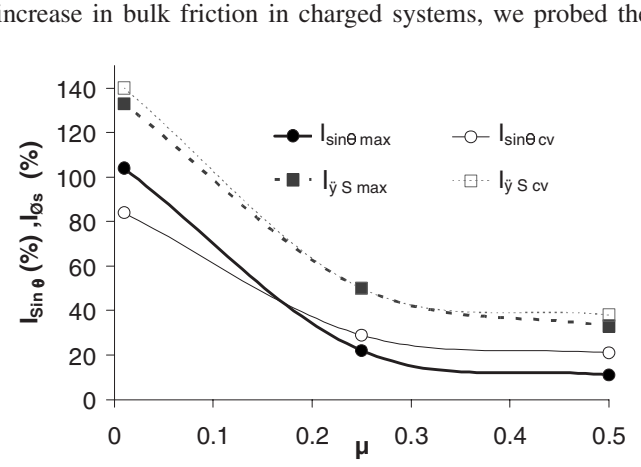

FIG. 4. Gain indices (I) measured at the peak $(\sin\theta_{\max}, \varnothing_{s\ \max})$ and steady state $(\sin\theta_{cv}, \varnothing_{s\ cv})$ conditions.

nature of force transmission characteristics [10–14,23–25] in our assemblies. Existing studies on force transmission characteristics in uncharged granular systems subjected to shearing show that, the load is transmitted by a relatively rigid, heavily stressed sparse network of contacts ("strong" contacts, some times their network is referred to as strong force chains) carrying greater than average normal contact force [e.g., [10–14,24,25]]. The remaining groups of particles, which separate the strong contacts, are only lightly loaded. Recent studies ($2d$ and $3d$) clearly indicate that the macroscopic strength characteristics of granular systems strongly depend on their ability to build-up strongly anisotropic fabric structure of strong contacts [e.g., [12,13,24]]. The directional orientation of the contacts are characterized, following the definition of "fabric tensor" $\varnothing_{ij}$, suggested by Satake [26] as $\varnothing_{ij}=\langle n_i n_j\rangle=\frac{1}{M}\Sigma_1^M n_i n_j$, where M is the number of contacts in the assembly and n_i is the unit normal vector at a contact between two particles. In the current study, we restrict $\varnothing_{ij}$ to a subset of the M contacts, viz. strong contacts (denoted by the suffix s). Irrespective of whether a granular system is charged or uncharged, our simulation results satisfied the equation $\sin\theta=\lambda(\varnothing_{s33}-\varnothing_{s11})$ throughout shearing, where λ is the scaling parameter. Nevertheless, it is possible to get similar relations between the bulk friction and the invariants of the fabric anisotropy tensor $\varnothing_{sij}$: we found that the following relations also satisfied the simulation data $\sin\theta=\lambda\sqrt{(\varnothing_{s33}/\varnothing_{s11})}$ and $\sin\theta=\lambda(\varnothing_{s33}/\varnothing_{s11})$ during all stages of shearing. We also observed that the scaling factor λ, is less dependant on the value of inter-particle friction between particles. This confirms our anticipation that the anisotropic orientation of the strong contacts significantly influences the bulk friction in both the charged and uncharged granular assemblies. This is further evident from the variation of I index for the fabric anisotropy tensor of the strong contacts ($I_{\varnothing s\,\max}$, $I_{\varnothing s\,\mathrm{cv}}$) as presented in Fig. 4. We observe that charging enhances the fabric anisotropy of strong contacts, more dominantly, in the case of low frictional granular systems. We also repeated all our simulations by reversing the direction of applied force to the adhesion force (i.e., the sign of the fourth term in F_{NE} is reversed)—yet the conclusions presented above did not change.

In summary, we analyzed the role of interparticle forces on the bulk friction and other key micromechanical properties of charged granular media subjected to slow shearing. We conclude that for dry (cohesive) granular systems charged in air, (i) the short range electrostatic forces between particles significantly contribute to the bulk friction—accounting for its variation over the separation distance between closest neighbors (grains) is essential, an aspect often ignored in the existing studies. The role of long-range electrostatic forces and pull-off force seems to be less influential towards the bulk friction in charged dense granular systems. These results would be helpful to industries to functionalize the interparticle forces and surfaces [7] to efficiently control the mobility of particulates in devices. (ii) Studies on dilation rate in charged system indicate that, at large deviatoric strain levels, granular bed expansion rate is less likely to be affected by charging. Hence, applying charging in combination with mechanical shearing (as often done) is not necessarily an effective way to mobilize granular beds. At large strain levels, charging could be terminated, thus leading to energy savings in powder/granular processing operations (iii) Charging enhances the fabric anisotropy of strong contacts, resulting in an increase in the bulk friction, more significantly, in the case of low frictional granular systems. The fabric-bulk friction correlations presented here provide a useful basis to describe the constitutive behavior of charged granular systems. The continuum description of granular material under such loading environments is not yet well established. The study presented here forms a basis, in order to account for more realistic situations in the future that are not considered here, such as the effects of thermal fluctuations between particles at small scales, the shape and size effects of the particles and the effects of other loading paths.

We thank Professor M. Kuhn, Dr. C. S. Hodges, and Dr. R. Moreno-Atanasio for their direct and indirect support to this study.

[1] H. M. Jager and S. R. Nagel, Rev. Mod. Phys. **71**, S374 (1996).
[2] F. Rajdai, H. Troadec, and S. Roux, in *Granular Materials: Fundamentals and Applications*, edited by S. J. Antony, W. Hoyle, and Y. Ding (Royal Society of Chemistry, London, 2004), p. 157.
[3] S. Masuda, J. Electrost. **10**, 1 (1981).
[4] G. S. P. Castle, J. Electrost. **51**, 1 (2001).
[5] D. S. Rimai, D. S. Weiss, M. C. Jesus, and D. J. Quesnel, Eureka **9**, 3 (2006).
[6] J. Q. Feng and D. A. Hays, Powder Technol. **135**, 65 (2003).
[7] W. Peukert *et al.*, Adv. Powder Technol. **14**, 411 (2003).
[8] A. K. Noor, in *Innovation in Engineering Computational Technology*, edited by B. H. V. Topping, G. Montero, and R. Montenegro (Saxe-Coburg Publications, Dun Eaglais, 2006), p. 1.
[9] A. Cundall and O. D. L. Strack, Geotechnique **29**, 47 (1979).
[10] S. J. Antony, Phys. Rev. E **63**, 011302 (2001).
[11] S. Ostojic, E. Somfai, and B. Nienhuis, Nature (London) **439**, 828 (2006).
[12] S. J. Antony and M. R. Kuhn, Int. J. Solids Struct. **41**, 5863 (2004).
[13] C. Thornton and S. J. Antony, Philos. Trans. R. Soc. London **356**, 2763 (1998).
[14] S. J. Antony and F. Sarangi, J. Comput. Theor. Nanosci. **3**, 1 (2006).
[15] J. Q. Feng, E. A. Eklund, and D. A. Hays, J. Electrost. **40**, 289 (1997).
[16] J. Q. Feng and D. A. Hays, IEEE Trans. Ind. Appl. **34**, 84 (1998).
[17] R. Jones and C. Hodges, in *Granular Materials: Fundamentals and Applications*, edited by S. J. Antony, W. Hoyle, and Y. Ding (Royal Society of Chemistry, London, 2004), p. 229.

[18] D. A. Hays, J. Adhes. **51**, 41 (1995).
[19] N. S. Goel and P. R. Spencer, Polym. Sci. Technol. **9B**, 763 (1975).
[20] D. A. Hays, J. Adhes. Sci. Technol. **9**, 1063 (1995).
[21] C. Thornton, Geotechnique **50**, 43 (2000).
[22] C. Goldenberg and I. Goldhirsch, Nature (London) **435**, 188 (2005).
[23] E. I. Corwin, H. M. Jaeger, and S. R. Nagel, Nature (London) **435**, 1075 (2005).
[24] F. Radjai, M. Jean, J. J. Moreau, and S. Roux, Phys. Rev. Lett. **77**, 274 (1996).
[25] T. S. Majmudar and R. P. Behringer, Nature (London) **435**, 1079 (2005).
[26] M. Satake, in *Deformation and Failure of Granular Materials*, edited by P. A. Vermeer and H. J. Luger (Balkema, Rotterdam, 1982), p. 63.